Development of the Laser-Induced Incandescence Method for the Reliable Characterization of Particulate Emissions

William D. Bachalo and Subramanian V. Sankar

Artium Technologies, Inc.

Sunnyvale, California

Gregory J. Smallwood and David R. Snelling

Combustion Research Group

Institute for Chemical Process and Environmental Technology

National Research Council, Canada

ABSTRACT

A laser-induced incandescence (LII) system has been developed for the non-intrusive and real-time measurement of soot particulate concentration and primary particle size, Fig.1. The LII system incorporates an innovative two-color pyrometry technique for accurate measurement of soot concentration. Furthermore, the LII signal decay characteristics are used to infer the primary particle size. Besides the self-calibrating feature, the instrument also uses low laser fluence and a top-hat laser beam for improved accuracy in the measurement. The system automatically maintains constant laser fluence over a wide range of environmental conditions and also attenuates the collected incandescence signal as needed to handle a large range of soot concentration. Another key feature of the instrument is its remote operation capability when it is connected to any computer network such as the Internet. This paper discusses the measurement technique, the instrumentation, and the experimental results obtained from a variety of applications including diesel and direct injection spark ignition automobile emission studies, and carbon black formation process in an industrial furnace.

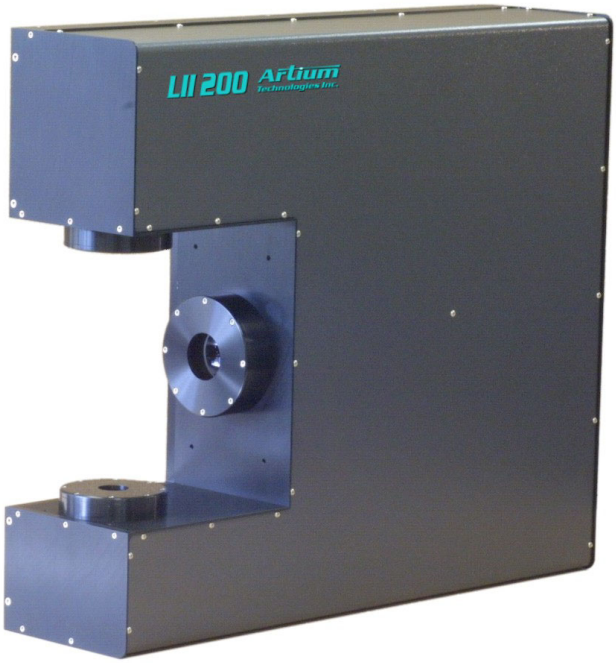

Figure 1: Photograph of the Artium LII system.

1. INTRODUCTION

Recent studies of the health effects of air pollution show that the levels of soot and other tiny particles found in large and midsize cities increase the risk of premature death from cancer and heart disease. Breathing high concentrations of lung-penetrating particulates has been shown by Arden et. al (2002) to be an important environmental risk factor for cardiopulmonary and lung cancer mortality. Studies by the American Cancer Society concluded that as the concentration of soot particulates increases, the risk of early death rises by 4 to 8 percent and increases the number of aggravated asthma cases, depending on the concentration and long-term exposure. Fortunately, soot particulates emitted by cars, trucks, power plants, factories, aircraft, and other combustion processes have been reduced substantially over the past decade and will drop further under pending regulations. However certain regions undergoing rapid industrial development are producing higher levels of particulate emissions. These emissions travel on the jet stream to produce a global rather than simply a national or urban problem. Not only the mass of the particulates but also the size and number density play a significant role in the health effects on humans and other living organisms as well as upon the climate.

Growing environmental concerns have raised the performance requirements of diesel-powered vehicles and aircraft gas turbine engines throughout Europe, North America, and Japan in an effort to reduce the level of particulate emissions. Tighter emissions controls on trucks and buses, and restrictions on off-road vehicles such as farm tractors and construction equipment will be implemented in the near future. Currently, certain stationary sources and off-road vehicles are unregulated. The problem is not a trivial one since diesel-powered vehicles, which are very fuel-efficient, are required in the transportation of goods and material to and from industrial operations and to consumers. The concession is that emissions reduction systems must be implemented in these vehicles in order to reduce pollutant formation and the emissions must be monitored to ensure adequate performance of the systems and compliance with regulations.

Particulate emissions from diesel engines are generally in the form of complex aerosols consisting primarily of soot and volatile organics. In terms of monitoring, currently, particulate matter emissions are defined as the mass of the matter that can be collected from a dilute exhaust stream on a filter kept at 52^{o} C. The method excludes condensed water but includes organic compounds that condense at this temperature or above. These measurements provide time-average PM emissions data for the period during which the particulates are collected on the filter. Transient PM measurements using this technique are impractical. Agglomeration of the collected PM and other condensed material occurs on the filter so the measurement of particulate size and size distribution may not be possible. Furthermore, as diesel engines improve, the quantity of PM generated is reduced, which pushes the gravimetric technique closer to its reproducibility and sensitivity limits, reducing the gravimetric technique to one of marginal utility.

Currently, particle size and number emissions from diesel engines are not regulated. At least two factors have led to this oversight: a general lack of instrumentation to adequately characterize the size and number of fine amorphous particulates; and the general lack of medical research evidence to define acceptable levels of PM as a function of aggregate size. However, the recent research cited above indicates that particulate levels existing in urban areas are producing significant hazards to our health. Furthermore, instrumentation developments are progressing that will allow more reliable and convenient means for characterizing the particulates that will lead to improved correlations between particular loading and expression of deleterious health effects.

2. LASER-INDUCED INCANDESCENCE

Laser-induced incandescence (LII) is rapidly emerging as a useful diagnostic for acquiring spatially and temporally resolved quantitative measurements of soot particle volume fraction over a very wide range of soot concentrations. Recent comparisons of the method have been made with the gravimetric sampling technique, Snelling et al. (1999), and there have been some successful measurements of the soot primary particle size, Snelling et al. (2000b). Since the identification of the phenomenon by Eckbreth (1977), laser-induced incandescence (LII) has undergone significant research and development as well as evaluation over a range of conditions and different applications. This method for measuring soot volume fraction and primary particle size produced by combustion systems has the advantages of offering a very wide measurement and dynamic range with a sensitivity estimated to be better than one part per trillion

(~2 μg/m^3). The measurements are made with high spatial and temporal resolution allowing in situ measurements of the time-resolved soot emissions.

Although the theory and analysis associated with the method, which involves nanosecond time response to nanoscale particles, is complex, the application of the method is relatively straightforward. With this technique, a pulsed laser with light pulse duration below 20 nanoseconds is used to rapidly heat the soot particles within the measurement volume from the local ambient temperature to close to the soot vaporization temperature (> 4000 K). Incandescence from the soot particles is detected by two detectors using appropriate line filters and the signals are recorded for subsequent analyses. Complex analysis of the nanoscale heat and mass transfer space and time are required in describing the laser light energy absorption by the soot particles and the subsequent cooling process. Although the method uses only laser light for heating and optical signal detection, and as such, is in situ and nonintrusive, it is not completely non-perturbing. Laser light heating of the soot may be expected to affect the soot morphology and produce some loss of particle mass due to evaporation.

LII has a well-defined but complex response to volatile particulate matter. It is totally insensitive to liquid particles, because they absorb a negligible amount of laser energy compared to carbon. For carbon particles coated with volatile material, the latter are believed to vaporize early in the laser heating period. In general, it is reasonable to state that LII measures the volume fraction of carbonaceous material in the exhaust. Although metallic ash may also be present at low concentrations, it has a low absorptivity and emissivity relative to carbon and is unlikely to survive the high temperatures, resulting in a negligible contribution to the incandescence.

The LII technique is capable of real-time measurements during transient vehicle operation, making it a valuable tool for optimizing gasoline and diesel engine soot emissions performance. The measurement frequency is only limited by the repetition rate of high-power pulsed lasers (typically 10-30 Hz, which corresponds to one measurement per engine cycle at 1200-3600 rpm). Therefore, while it is not possible to obtain crank-angle resolution in real-time, ensemble-averaging for many engine cycles can be used to reconstruct cycle-resolved transient behavior. However, the real-time measurement frequency is more than adequate to observe engine and vehicle transients, such as those that occur in driving cycles.

LII measurements generally provide a relative measure of the soot volume fraction and thus, a means for calibration is required to relate the signal to the soot concentration. Previously, a comparison of the LII results to a system with a soot volume fraction measured by traditional methods was used to calibrate the instrument. The method was inconvenient and not practical for routine applications of the diagnostic. A novel method has been developed using absolute light intensity measurement that avoids the problem of calibrating with a known source of soot particles [Snelling et. al. (2000a), Snelling et. al. (2001)]. This in situ absolute intensity approach has been used with the LII method while measuring soot volume fraction in laminar diffusion flames, carbon black, diesel engine exhaust, and direct injection spark ignition (DISI) engine exhaust [Smallwood et. al. (2001b)]. Coupled with additional work on the definition of the spatial and temporal characteristics of the sample volume, results obtained from diesel and spark ignition showed improved reliability.

In the following sections, the state-of-the-art model describing nanoscale (time and space) heat transfer to and from the soot particles will be presented, the approach used for measuring soot volume fraction and primary particle size will be discussed, and representative experimental results showing the recently developed capabilities will be presented and discussed.

THEORETICAL HEAT TRANSFER MODEL

Soot (elemental carbon based particles emitted from combustion sources) absorbs and emits light predominantly on the scale of the primary particles. Conventionally, a high-energy pulsed laser beam is used to rapidly heat the soot particles from the local ambient temperature to the carbon vaporization temperature (~ 4000 K). The laser heating process is independent of particle size, and the emitted light is nominally volumetric, when the following assumptions apply: (1) soot primary particles are small compared to the laser wavelength (Rayleigh regime); (2) laser heating increases the temperature of all particles at the same rate, regardless of size; (3) when the particles reach the vaporization temperature, additional absorbed energy goes into vaporization rather than sensible energy, so that the particles remain

at the same temperature for the duration of the laser heating period; (4) vaporization causes negligible particle-size reduction, so that the incandescent radiation from the particles is independent of laser fluence above the vaporization threshold.

Significant work has been devoted to the theoretical modeling of the transient soot heating and cooling characteristics going back to the work of Melton, (1984) and others. The analysis outlined follows the work of Snelling, et al. (1997) who improved upon the analyses of Hofeldt (1993). Soot particles are described as aggregates of N_p soot primary particles of diameter d_p, as suggested by Dobbins and Megaridis, (1987) that are just touching. The heat transfer model considers isolated primary particles. The heat transfer equation for the energy balance for a transient heated (by 10 ns laser light pulse) soot particle is given as

$$C_a q - \frac{2k_a(T-T_0)\pi d_p^3}{(d_p + G\lambda_l)} + \frac{\Delta H_v(T)}{M_v(T)}\frac{dM}{dt} + q_{rad} - \frac{\pi d_p^3}{6}\rho_p c_p \frac{dT}{dt} = 0 \tag{1}$$

The first term represents the absorbed laser light energy by the soot aggregate where q is a function describing the laser intensity in W/cm^2 and C_a is the soot absorption cross section. The last term is the laser heating where ρ_p is the soot density (kg/m^3) and c_p is the specific heat of the carbon particles.

In this analysis, the soot aggregates are taken as an agglomerate of just touching primary spheres of nearly monodisperse diameter d_p that are well within the Rayleigh limit. Furthermore, the absorption coefficient C_a for the soot is expressed as follows:

$$C_a = \frac{\pi^2 d_p^3 E(m)}{\lambda} \tag{2}$$

where the complex refractive index is $m = n + ik$ and

$$E(m) = -\,\mathrm{Im}\left[(m^2 - 1)/m^2 + 2)\right] \tag{3}$$

and so

$$E(m) = \frac{6nk}{(n^2 - k^2 + 2)^2 + 4n^2k^2} \tag{4}$$

For a wavelength of 1064 nm and a refractive index obtained from the dispersion relationship from Dalzell and Sarofim is $m = 1.63 + 0.7i$ and E(m) = 0.30 while at 532 nm, $m = 1.59 + 0.58i$ and E(m) = 0.26.

The second term in Eq. (1) describes the heat transfer to the surrounding medium, specified in terms of the aggregates of primary particles. In the expression, G is a geometry dependent heat transfer coefficient specified as

$$G = \frac{8f}{\alpha(\gamma + 1)} \tag{5}$$

where f is the Eucken factor equal to 5/2 for monatomic species, α is the accommodation coefficient now assumed to be ~0.26, $\gamma = c_p/c_v$ (=1.4 for air) is the ratio of specific heat coefficients. Snelling, et al. (1997) reported the work of Leroy, et al. (1997) in which they made measurements indicating that the accommodation coefficient of nitrogen on solid graphite in the temperature range of 300 to 1,000^{o}K gave a value of 0.26. Snelling et al. found that the previous

analyses with an accommodation coefficient of 0.9 incorrectly predicted the very fast decay in the LII signal whereas the value of 0.26 gave good agreement with the experiment.

The expression describes the heat transfer to the surrounding medium in the case of the transition regime between free molecular and a continuum. However, the soot aggregates are generally smaller than the molecular mean free path length in the typical flame environments. That is, the Knudsen number, $K_n = l / d_p$ is much greater than 1 and hence, the heat transfer coefficient is independent of the particle size. It should also be noted that in the denominator, $Gl >> d_p$ so the dependence of the soot particle diameter becomes insignificant in this term.

The third term in the Eq.(1) describes the loss of heat from the particle due to evaporation of the carbon. The rate of mass loss is given by the analysis of Hofeldt (1993) assuming that the particle surface is essentially stationary and that the vapor is lost by diffusion is given as

$$\frac{dM}{dt} = \frac{\rho_p}{2}\pi d_p^2 \frac{dd_p}{dt} = -\frac{\pi d_p^2 N_v M_v}{N_{AV}} \tag{6}$$

where N_v is the molecular flux of evaporating carbon vapor for the free molecular condition (K_n>>1), M_v is the soot vapor molecular weight and N_{AV} is Avogadro's number.

The fourth term in Eq.(1) describes the radiative heat loss by a primary particle given as

$$q_{rad} = 4\pi^2 \sigma_{SB} T^4 \left(\frac{E(m)}{\lambda} \right) \tag{7}$$

where the parenthetical expression is evaluated at the wavelength of interest. Compared to the other heat loss mechanisms, the heat loss due to radiation is insignificant.

The last term in Eq.(1) which is

$$\frac{\pi d_p^3}{6} \rho_p c_p \frac{dT}{dt}$$

describes the particle heating.

Identification of errors propagated through the literature has led to further development of this state-of-the-art numerical model of nanoscale (time and space) heat transfer to and from the particles, in order to support understanding of the physical processes occurring during the LII event [Smallwood et al. (2001a)]. This model has been enhanced to the point where it will well predict the time-resolved behavior of the LII signals for a range of laser fluences.

QUANTITATIVE CONCENTRATION MEASUREMENTS

The standard practice for measuring soot volume fractions is to calibrate the LII systems in a steady-state flame using extinction measurements. Recently, however, a novel technique for performing absolute light intensity measurements in LII has been presented, thus avoiding the need for a calibration in a source of soot particulates with a known concentration [Snelling et. al. (2000a), Snelling et. al. (2001)], and thus extending the capabilities of LII for making practical quantitative measurements of soot. The use of the absolute intensity approach provides for continuous *in situ* self-calibration of the LII technique, and allows use of lower laser fluences and lower maximum soot temperatures. This low fluence approach simplifies interpretation of the data and lessens the burden of the assumptions noted above. Thus, issues associated with evaporating a significant portion of the soot are avoided. The absolute intensity method,

or self-calibrating LII, is a time-resolved approach that applies two-color pyrometry principles to determine the particle temperatures, relating the measured signals to the absolute sensitivity of the system as determined with a strip filament lamp.

Self-calibrating LII is based upon knowledge of the particulate surface temperature, determined by optical pyrometry. If two or more independent wavelengths, λ, are recorded, an average soot particle surface temperature across the laser sheet can be calculated by using the ratio of the observed signals (corrected for detection sensitivity) and the known soot particle absorption cross sections. A single point calibration is made with a known radiance source, which provides calibration factors, η(λ), to relate the measured signals to the absolute spectral intensities of the source (in $W/m^3 \cdot ster$)

$$\eta(\lambda) = \frac{V_{CAL}(\lambda)}{R_S(\lambda, T)} \tag{8}$$

where $V_{CAL}(\lambda)$ is the observed signal from the calibration lamp and $R_S(\lambda,T)$ is the spectral radiance of the lamp. The calibration factor η accounts for the collection efficiency of the receiver and the detector responsivity at the detection wavelength λ.

Using the previously described heat transfer model, the power radiated by a single particle of diameter d_P into 4π steradians can be expressed as (see, e.g. Snelling et al. (2000c))

$$P_p(\lambda) = \frac{8\pi^3 c^2 h}{\lambda^6}\left(e^{\frac{hc}{k\lambda T}} - 1\right)^{-1} d_p^3 E(m_\lambda) \tag{9}$$

where $E(m_\lambda)$ is a refractive index dependent absorption function, h and k are Planck and Boltzmann constants, respectively, c is the velocity of light, and T is the particle temperature. The spectral radiance of the soot is dependent upon the power radiated by a single particle, $P_p(\lambda,T)$ and the number of particles in the probe volume, N_p. $N_p = n_p(w_b A_p)$, where n_p represents the concentration of primary particles in the probe volume, and the quantity in parentheses represents the volume interrogated, with w_b as the equivalent width of the laser sheet and A_p is the cross-sectional area of the probe volume, as viewed by the detection system. The equivalent width of the laser sheet must be measured experimentally. As this area is the same for both the calibration and the particle measurement, an equivalent spectral radiance for the particles in the probe volume, R_p, can be defined as

$$R_p(\lambda) = \frac{P_p(\lambda) n_p w_b}{4\pi} \tag{10}$$

which can be related to the observed signal from the particles, $V_{EXP}(\lambda)$, by the calibration factor, η(λ), such that

$$\eta = \frac{4\pi \cdot V_{EXP}(\lambda)}{P_p(\lambda) n_p w_b} \tag{11}$$

The observed signal ratio at the two wavelengths $V_{EXP}(\lambda_1)/V_{EXP}(\lambda_2)$ can be converted to relative particle radiance using the calibration factors

$$\frac{P_p(\lambda_1)}{P_p(\lambda_2)} = \frac{V_{EXP}(\lambda_1)}{V_{EXP}(\lambda_2)} \frac{\eta(\lambda_2)}{\eta(\lambda_1)} \tag{12}$$

The ratio of the powers at two wavelengths radiated by a single particle is given by

$$\frac{P_p(\lambda_1)}{P_p(\lambda_2)} = \frac{\lambda_2^{\,6}}{\lambda_1^{\,6}} \frac{\left(e^{\frac{hc}{k\lambda_2 T}} - 1\right)}{\left(e^{\frac{hc}{k\lambda_1 T}} - 1\right)} \frac{E(m_{\lambda_1})}{E(m_{\lambda_2})} \tag{13}$$

Using the experimentally determined power ratio from Eq. (12), the known values of $E(m_\lambda)$, and assuming all the particles in the probe volume are heated to the same temperature, Eq. (13) can be solved for T. It is the relative, not the absolute, magnitude of the particle absorption function at the two wavelengths that is important in determining soot particle surface temperature. For the work presented here, the values for $E(m_\lambda)$ were those determined by Krishnan *et al.* (2001).

The particle (soot) volume fraction is given by

$$f_v = n_p \cdot \frac{\pi\, d_p^{\,3}}{6} \tag{14}$$

Expressing Eq. (9) in terms of $d_p^{\,3}$, and Eq. (11) in terms of n_p, and substituting into Eq. (14), the soot volume fraction is then

$$f_v = \frac{V_{EXP}(\lambda)}{\eta(\lambda)\, w_b} \frac{\lambda^6 \left(e^{\frac{hc}{k\lambda T}} - 1\right)}{12\,\pi c^2 h\, E(m_\lambda)} \tag{15}$$

The soot volume fraction has an inverse dependence on the absolute magnitude of the particle absorption function.

Differences between the volume concentration of soot measured with LII and the total PM measured with other techniques can be attributed to several factors. These factors include: uncertainty in relating soot volume fraction to the relevant property of the PM measured by the other techniques; uncertainties in the LII technique; and uncertainty and errors introduced by the other techniques.

The uncertainties in the absolute intensity approach to LII are primarily due to uncertainty in the soot refractive index at elevated temperatures. In particular, one must know the relative value of $E(m_\lambda)$ at the two wavelengths to correctly determine the temperature, and the absolute value of $E(m_\lambda)$ to determine the concentration once the temperature has been determined. For the results presented, the relative value of $E(m_\lambda)$ at the two wavelengths based on the best available data of Krishnan *et al.* (2001) is increasing ~20% with wavelength over the range 400 nm – 800 nm. However, recent results from our own work , Snelling et al., (2002), indicate that over the visible to near-infrared range the relative value of $E(m_\lambda)$ is constant. Sensitivity analysis indicates that a change in the relative value of $E(m_\lambda)$ of this magnitude will result in an increase in the soot volume fraction of the order of 50%. Similarly, sensitivity analysis on the absolute value of $E(m_\lambda)$ indicates a 1:1 correspondence, such that a 20% uncertainty in the magnitude of $E(m_\lambda)$ leads to a 20% uncertainty in the soot volume fraction. Furthermore, $E(m_\lambda)$ may vary with temperature as the soot structure may be altered as it is heated by LII, and the presence of SOF may also affect the soot absorption function.

A minor uncertainty which also affects the accuracy in a systematic manner is in the knowledge of the effective center wavelength of the detection system for each of the two wavelengths. As the temperature of the source changes, whether it is the calibration lamp or the heated soot particles, the effective center wavelength of the combination of the dichroic mirror, interference filter, and detector response varies in a nonlinear yet predictable manner. This systematic inaccuracy is greatest for short wavelengths, low temperatures, and large bandwidths, reducing monotonically with increasing temperature. It is less than 5% for the data presented. This inaccuracy could be corrected for with an

iterative approach to the data analysis, which was deemed unnecessary with respect to the negligible effect on the results.

PRIMARY PARTICLE SIZE

Immediately after the laser pulse, the dominant cooling mechanism for the particles is conduction to the surrounding gas. Assuming monodisperse primary particles, the temperature difference between the particles and the ambient gas decays steadily in an exponential manner during this period. An equation of the form

$$\Delta T = A \cdot e^{-\frac{\Delta t}{\tau}} \tag{16}$$

where a constant, A, is fit to the temperature data to determine τ, the time constant of the exponential decay. This method requires *a priori* knowledge of the ambient gas temperature, which may be determined by thermocouple.

The particle diameter d_p is then determined from the relation

$$d_p = \frac{12 k_g \alpha}{G \lambda_{MFP} c_p \rho_p \tau} \tag{17}$$

where k_g is the thermal conductivity of the ambient gas, α is the accommodation coefficient, G is a geometry-dependent heat transfer coefficient, λ_{MFP} is the mean free path in the ambient gas, and c_p and ρ_p are the specific heat and density of the particle, respectively.

Because the primary particle size determined from the cooling rate is proportional to the surface area per unit volume (specific surface area) available for conduction, it is an effective or *apparent* size. With our approach, we treat the particles as individual monosized primary particles, not accounting for the effects of size distribution and aggregation. Due to shielding and bridging of particles in an aggregate, the available specific surface area is substantially reduced, resulting in an apparent primary particle size that is significantly *larger* than the size one would measure with techniques such as transmission electron microscopy (TEM). From unpublished work, we have found that our measurements of the apparent primary particle size are on the order of two times greater than the actual primary particle size. Although acknowledged, this issue is not treated at this time.

Another significant uncertainty is the accommodation coefficient, which is often ignored (assigned a value of 1) or assigned a textbook value of 0.9, which may be suitable for equilibrium conditions at room temperature. We use the value of 0.26 determined by Leroy et al. (1997) which is the only measurement we are aware of for carbon under nonequilibrium conditions at elevated temperatures. However, it is unclear whether this value is valid for the full range of temperatures that we encounter.

3. LII SYSTEM

A fully-integrated, portable LII system has been developed for soot particulate characterization in various applications. A schematic layout of the Artium LII system is presented in Fig. 2. This system consists of a pulsed Nd:YAG laser, operating with 60 mJ/pulse at 20 Hz and 1064 nm. A half-wave plate (to rotate the plane of polarization) in combination with a thin film polarizer (angle-tuned to transmit horizontally polarized radiation) is used to adjust the laser energy as required. A second half-wave plate is used to return the plane of polarization to vertical. True top-hat profiles are used for all measurements to deliberately ensure that the soot particles are heated to a uniform temperature throughout the sample volume. As a result, there is no direct need to apply the numerical model described earlier in the analysis of LII signals. Low fluence LII, ~0.1 J/cm^2, is employed to limit the peak soot temperatures to ≤4000 K, ensuring that negligible soot evaporation occurs. A photodetector is used to measure the transmitted laser energy and the polarizer is automatically adjusted to maintain the desired fluence from pulse-to-pulse.

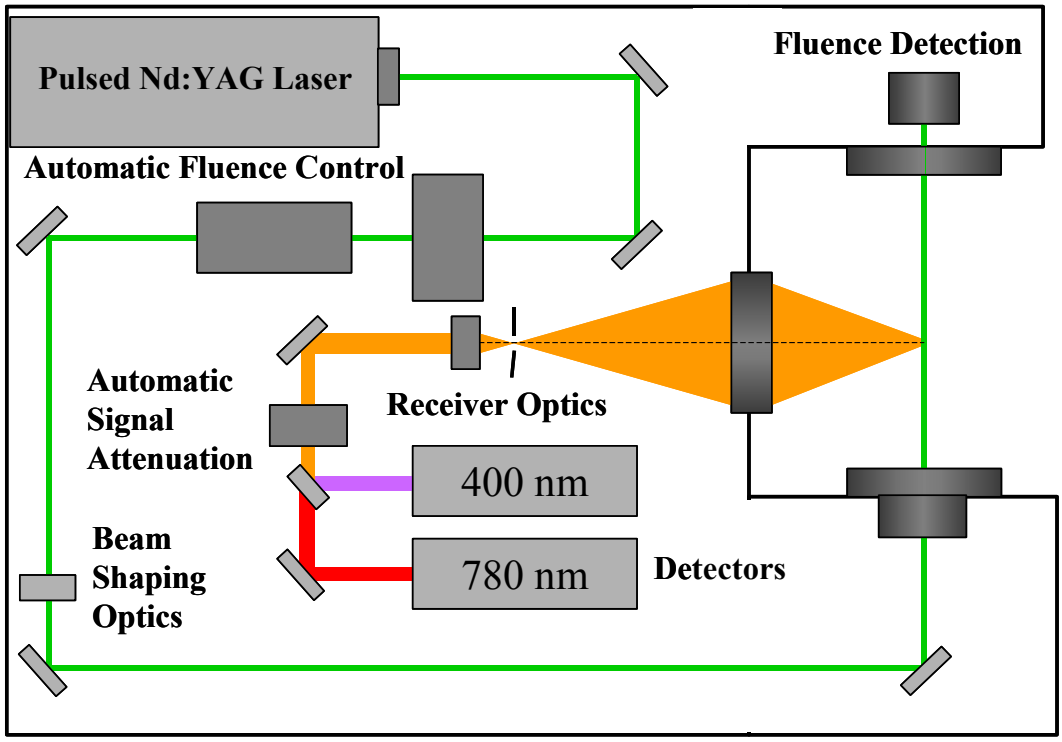

Figure 2: Schematic layout of the Artium LII system.

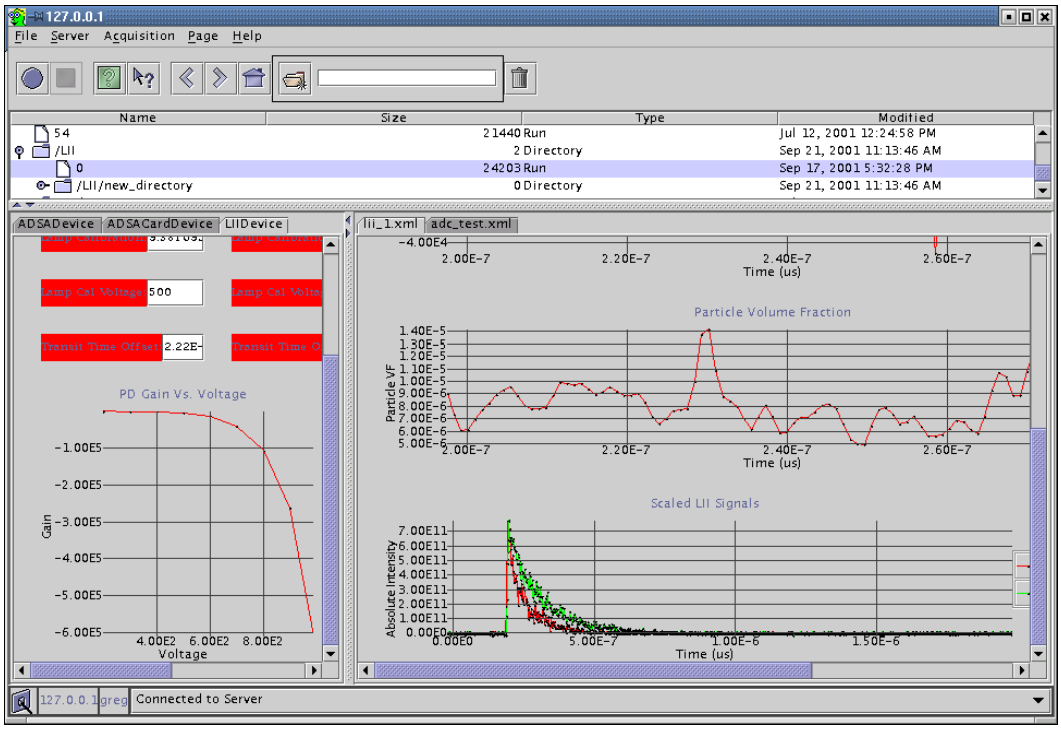

Figure 3: Typical system screenshot showing LII decay signals and computed soot volume fraction.

The LII signal from the center of the laser beam is imaged at 1:1 magnification onto a 2 mm diameter aperture, which is direct-coupled to a two-channel color separation and detection unit. The imaging system is arranged such that the imaging axis is at an angle of 90º from the forward direction of the laser beam. The collected LII signal is color separated and independently recorded by two photomultipliers, equipped with narrowband interference filters centered at 400 nm and 780 nm, respectively. An automatic light attenuation system is incorporated to provide for wide dynamic range detection. The transient signals from the photomultipliers are recorded by a high speed data acquisition board and subsequently transferred to a computer for further analysis. Figure 3 shows a typical system screenshot showing the LII decay signals and computed soot volume fraction.

4. RESULTS AND DISCUSSION

Before discussing the experimental results, it may be instructive to provide a brief description of the morphology of soot. As seen in Fig. 4, soot consists of large chain like aggregate of nearly spherical primary particles fused together. The soot primary particles are about 20 to 50 nm in diameter. Clearly it would be absurd to attempt to describe the light scattering by such particles using the Lorenz-Mie theory.

Diesel engine generated particulate matter consists of solid fraction, a soluble organic fraction (SOF), and sulfates. The analytic technique used to extract the organic fraction from the carbonaceous material leads to the adjective " soluble". The soluble organic fraction and the sulfates are generally referred to as the volatile organic fraction (VOF). The solid fraction is essentially carbon consisting of molecules of C/H ratios ranging from 4 to 11 with a density of approximately 2 g/cc. SOF includes polycyclic aromatic hydrocarbons (PAH), which have benzene rings joined in various forms. PAH is a possible carcinogen and may be the major cause of the health risk fears for particle emissions from diesel engines since their very small and can penetrate deep into the alveoli and are embedded in the lung tissue. There is additional salt material that occurs in the form of metal ash compounds derived from lubricating oil when dealing with diesel generated soot particulate.

Figure 5 shows a typical LII signal obtained in a laminar diffusion flame [Snelling et al. (2001)]. The incandescence signal varies as a function of time exhibiting a rapid rise caused by the heating of the soot particles by the laser followed by a relatively slower decay as the particles cool to the ambient temperature. The curves shown are for the 400 nm and 780 nm detector wavelengths used in the instrument. The longest wavelength (780 nm) can be observed to be the first to rise following the initiation of the laser pulse and is also the slowest to decay. The black body emission is shifted towards blue wavelengths at higher temperatures and has a faster decay due to the temperature dependence of the incandescence signal. The time basis for the two signals were adjusted for the difference in time constants of the photomultiplier tubes, cable lengths, and other variations in the system. Figure 6 shows the signal for a lower particulate concentration of only 0.4 ppb (0.76 mg/m^3) but the signal-to-noise ratio is still sufficient to accurately process the signal.

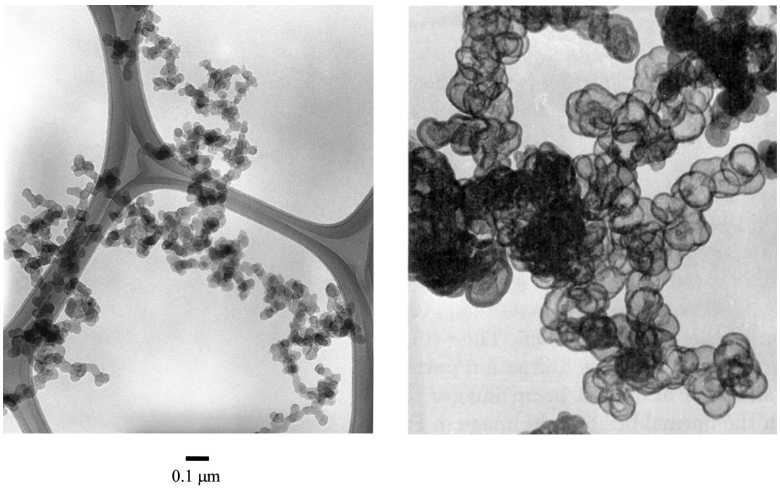

Figure 4: Transmission electron microscopy (TEM) images of soot collected on a filter from a diffusion flame.

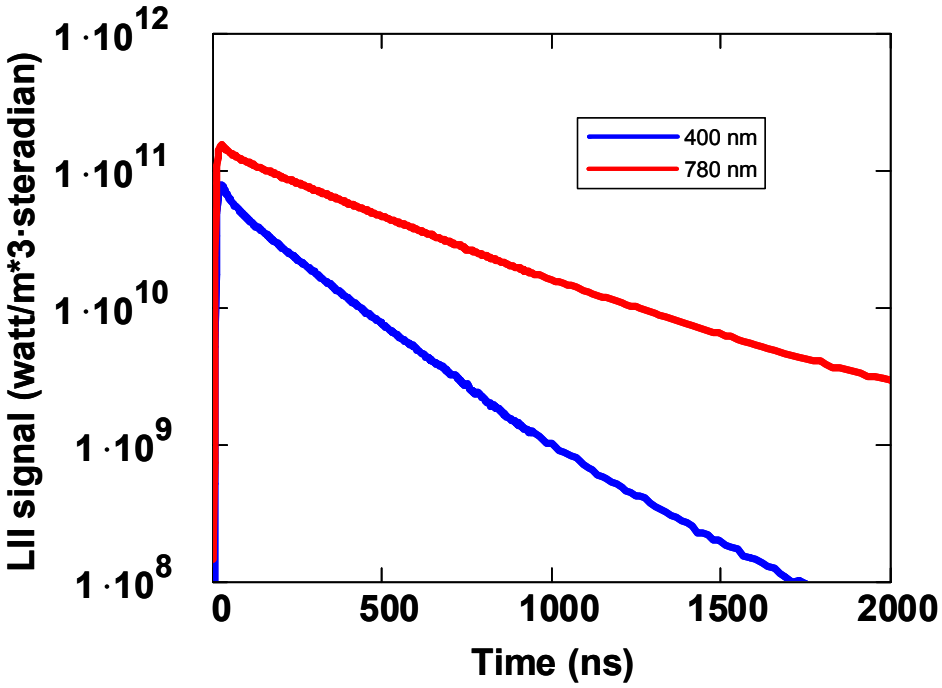

Figure 5: Characteristic LII signals for the two wavelengths used in the instrument.

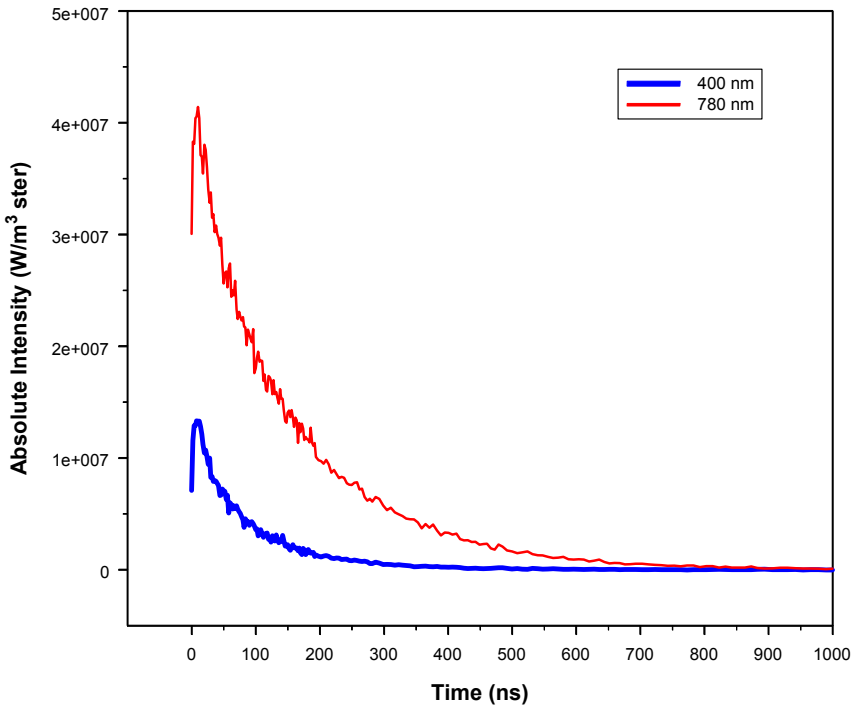

Figure 6: Typical LII signals for 400 nm and 780 nm detectors for a single acquisition, illustrating signal quality for moderate concentration (400.0 ppt) decays as particles cool to ambient temperature.

SOOT PARTICULATE SURFACE TEMPERATURE

The time-dependent particulate surface temperature was measured using the optical pyrometry technique throughout the rapid heating phase and the subsequent cooling phase of the particles. The precise measure of the particulate surface temperature was obtained using the LII technique for periods from shortly after the peak to when the signal had dropped by more than two orders of magnitude. Figure 7 presents typical temperature data obtained in a diesel engine exhaust, Snelling et al. (2000c). Temperatures as high as 4400 to 4500 K were typically observed. Measurements of concentration of particulates were determined from the maximum absolute intensity of the LII signal and the peak particulate surface temperature, Fig. 8. Linearity observed in the calibration curve was shown to be approximately within a single standard deviation of the best-fit line over almost two orders of magnitude.

As previously indicated, comparison of the particulate concentration data obtained from LII via the absolute calibration method was in good agreement with gravimetric data acquired simultaneously as shown in Fig. 9. The AVL steady-state simulation of the EPA transient test procedure was used in this example. Under this protocol, engine emissions were measured at steady speed/load conditions. The engine was varied from a low idle speed (600 RPM / 0 percent load) to the engine's rated speed and load (1800 RPM / 100 percent load). A weighting scheme used was designed to produce composite brake specific emissions to accurately predict the gaseous omissions obtained using the EPA transient test procedure. Since steady-state simulation does not accurately simulate transient engine behavior, these composite PM emissions can only be expected to show the current trends due to engine transients. Some of the discrepancies in the data may be attributed to the fact that gravimetric sampling includes an organic fraction that does not contribute to the signal measured by LII and density of the particulates is required to convert the mass determined by the gravimetric filter methods to volume fraction for comparison with LII.

Comparisons were also made between the LII instrument and the AVL smoke meter for the eight engine modes in the EPA simulation. The results shown in Fig. 10 indicates very good correlation between the two measurements over 2.5 orders of magnitude variation in soot concentration. The solid line in Fig. 10 represents the regression fit to the data and the dashed line represents perfect agreement between the two methods. Numbers on the graph indicate the data points for each mode of the AVL 8-mode simulation.

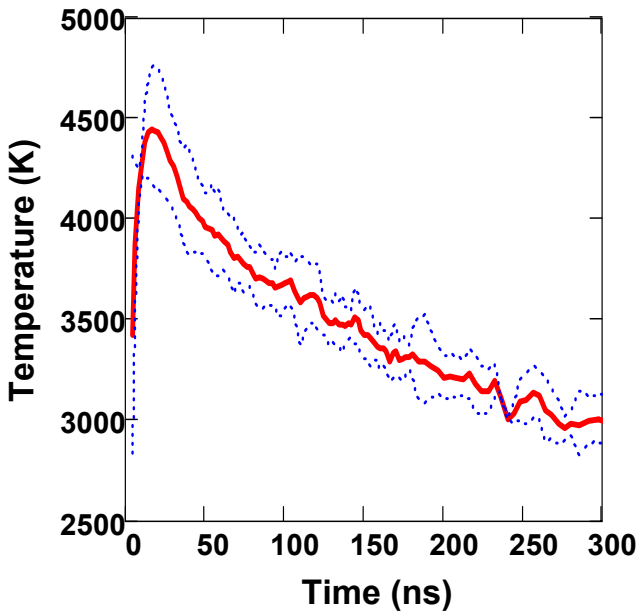

Figure 7: Soot surface temperature measured from the LII decay signal in a diesel engine exhaust.

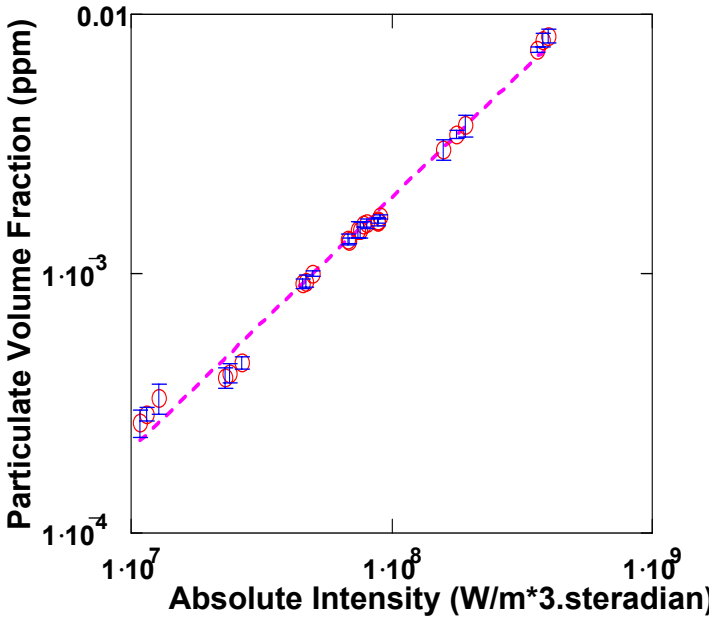

Figure 8: Particulate volume fraction as determined from absolute intensity of LII signal in diesel exhaust.

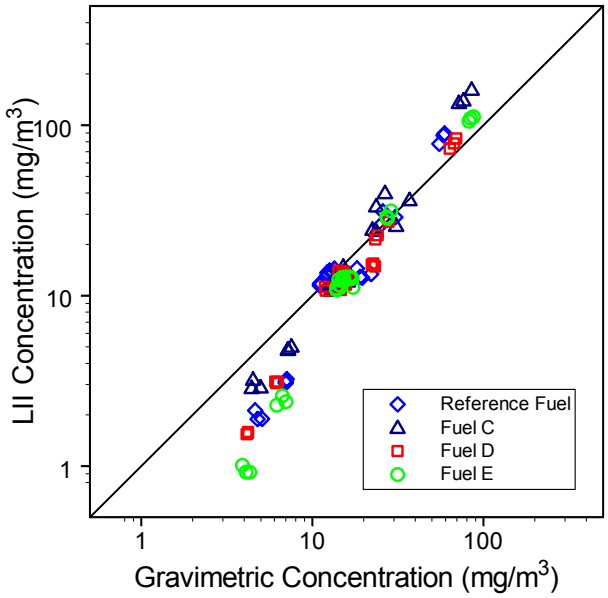

Figure 9: Soot particle concentration determined by the LII and gravimetric methods concurrently, for four different fuels.

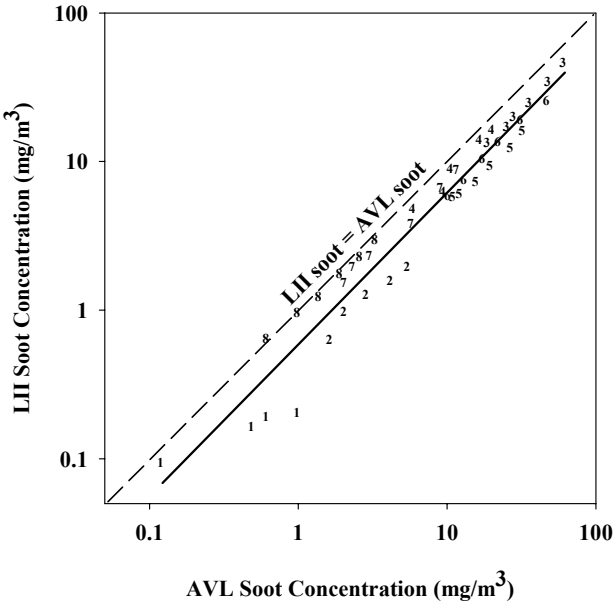

Figure 10: Comparisons of the soot concentration measured with the LII instrument and the AVL smoke meter for the AVL steady-state simulation.

PRIMARY PARTICLE SIZE

After the laser excitation, the particle cooling mechanism is dominated by conduction to the surrounding gas. During this conduction phase, the temperature difference between particle surface and the ambient gas decays steadily in an exponential manner. The surrounding gas temperature may be obtained from a thermocouple measurement or other means. As discussed earlier, the primary particle size may be obtained from this rate of decay of the LII signals, Fig. 11. Figure 12 shows the relationship between the particle size and the characteristic time of the exponential decay.

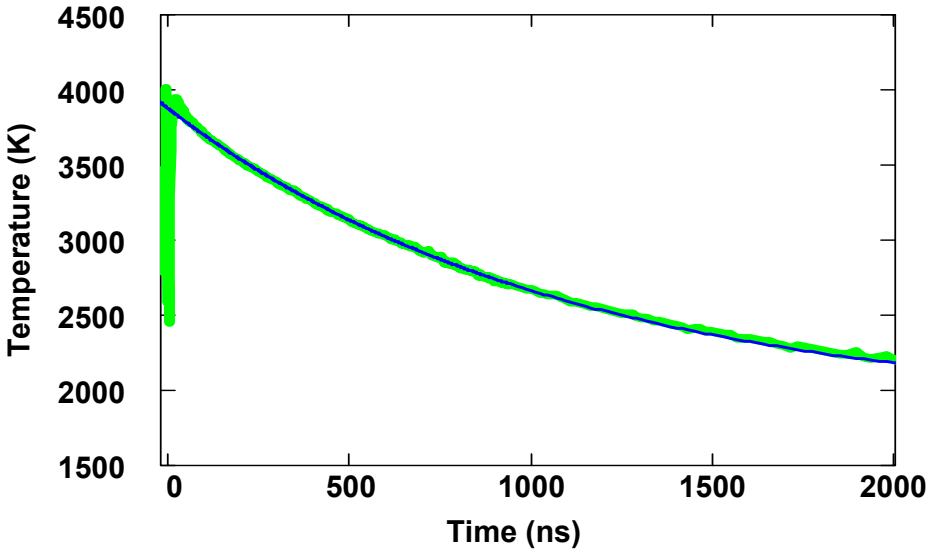

Figure 11: Example of the LII signal decay shown with an exponential fit to the results.

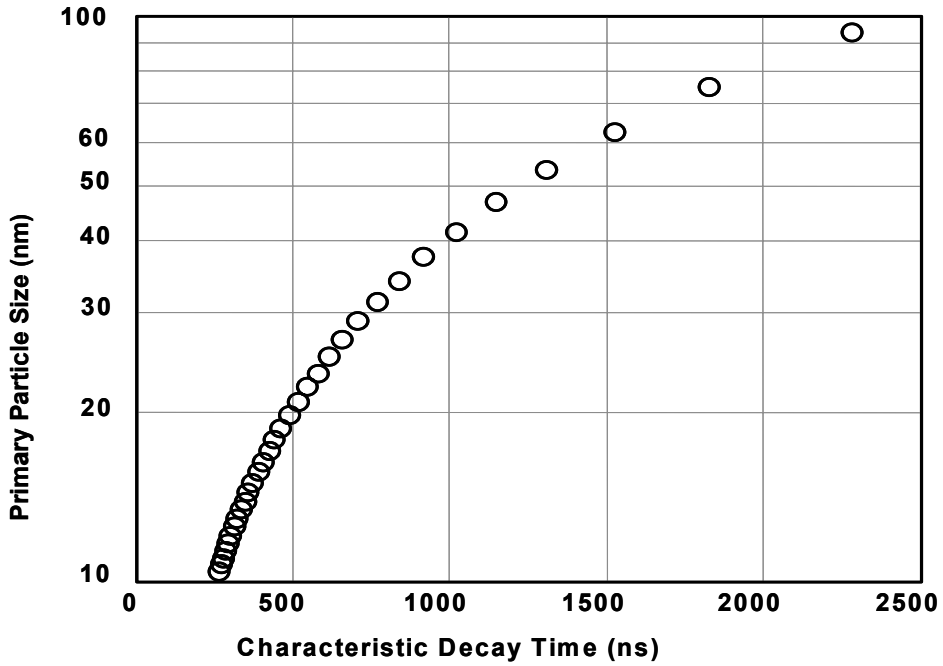

Figure 12: Relationship between the particle size and the characteristic time of the exponential decay for a range of primary particle sizes.

Another example of primary particle size measurements obtained for dispersed carbon black powders is shown in Fig. 13. These results were obtained for various operating conditions of the carbon black production furnace. The results clearly show that small changes in the primary particle size may be detected using the LII method. Measurements at two conditions showed very narrow size distributions and were consistent with the data obtained by other means. These data indicate that the LII method will be a useful tool for monitoring the formation of carbon black for industrial applications.

TRANSIENT SOOT EMISSIONS MEASUREMENTS

Suitable means for reliably measuring the various soot-related parameters entails the development of a system with an adequate dynamic range in order to monitor and characterize pollutant emissions over a wide range of concentrations. The system must also operate under a range of environmental conditions from in situ exhaust to atmospheric monitoring. Currently, gravimetric and other systems used in particulate emissions monitoring require dilution of the exhaust gas before making measurements. There are significant concerns regarding the effects of residence time, dilution ratio, sample temperature, preconditioning, collection and entrainment within the sampling lines when using a sampling approach. There are also concerns with instruments currently used to measure particulates. These issues have been summarized by Witze (2001).

To demonstrate the LII technique's capability for measuring transient emissions, data were obtained from a state-of-the-art production direct injection spark ignition engine. The unmodified engine used a lean burn stratify charge combustion concept for most of its operating modes and all emissions were measured from the tailpipe. A series of driving cycles were applied including the Cold Start (CS) LA-4 transient driving cycle, the Hot Start (HS) LA-4 transient driving cycle, and the HWFET (Highway fuel economy tests) transient driving cycle. This research was performed on the chassis dynamometer normally used for regulatory compliance testing, equipped for EPA FTP emissions measurements. Gravimetric filter sampling was performed to measure $PM_{2.5}$ mass emissions rate and particle phase organic carbon/elemental carbon content, sulfate content, and to collect samples for detailed organic analysis.

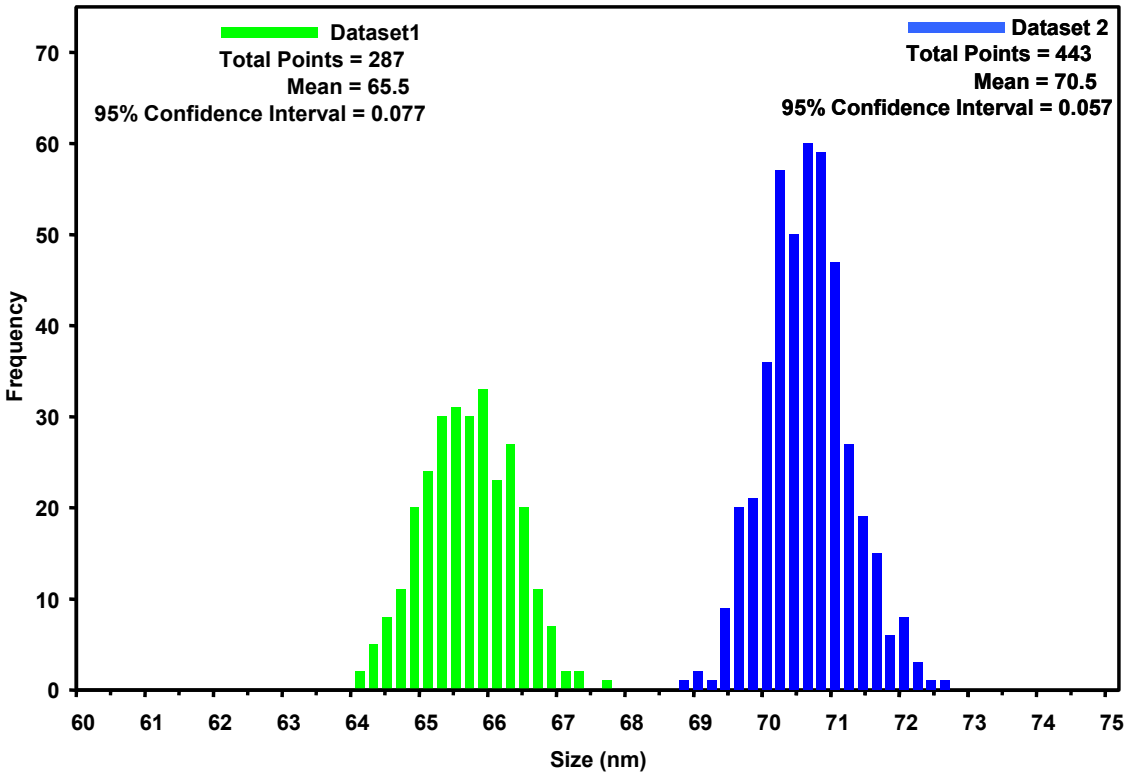

Figure 13: Primary particle size measured for carbon black formation for two different furnace operating conditions.

A fixed dilution ratio Dekati mini-diluter was used to sample the exhaust gas and direct it into the ELPI (electric low pressure cascade impactor) instrumentation for obtaining particulate size distributions. Samples were drawn from the exhaust hose at a point within 1 m of the tailpipe exit and conveyed through a heated sampling line (100^{o} C) to the diluter. A Dekati ELPI was used for the size distribution measurements. The ELPI produces data at 1-second intervals, for a limited number (12 stages) of size bins.

Dilution was unnecessary for the LII method since it responds to only the carbonaceous component of the particulates. Any condensed material including the organic fraction of the particulates and water do not contribute to the measured LII signal. The high-energy laser typically evaporates these volatile materials well before the significant portion of the LII signal is detected. The windows of the LII system were monitored for contamination but did not require cleaning, due to the low level of particulates being sampled and the low airflow through the cell that served to purge the windows. The exhaust gases were drawn through the cell at a constant 5 SLPM flow rate, which resulted in a transit time of the particulate through the sample line of approximately 6 seconds.

LII measurements of PM mass emissions rates for two cold start LA-4 trials obtained on consecutive days are shown in Fig. 14. The upper plots show the particulate mass emissions and the lower plots shows the vehicle speed. Clearly, the greatest soot mass emission rates occur during the first 50 seconds of this cycle. During this time the engine and emissions systems are warming up and consequently, not functioning at full performance. Subsequently, the increased mass emissions rate episodes for this engine correspond to the acceleration phases. After the warm-up period, deceleration and relatively steady driving speeds produce minimal levels of carbonaceous particles, and even during acceleration, these levels do not reach 1 mg/m^3. Although there is some variation in the PM emissions on a trial-to-trial basis, the results clearly track each other and transients in the driving cycle.

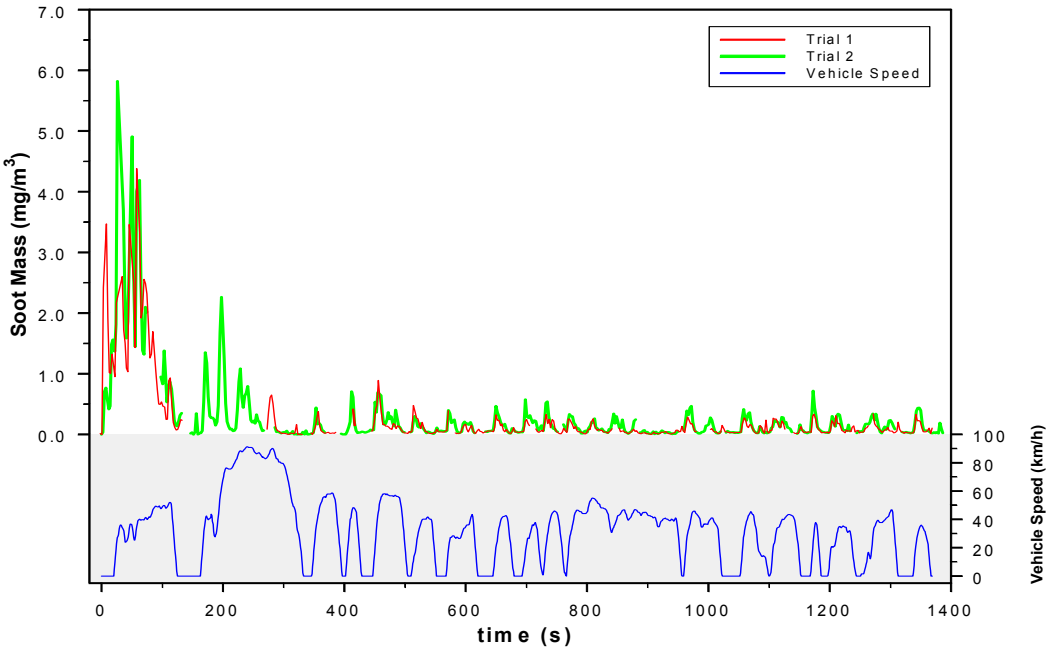

Figure 14: Comparison of cold start LA-4 transient cycle particulate mass emissions as determined by LII for two separate trials (top) and vehicle speed during LA-4 transient cycle (bottom).

For the hot start LA-4 driving cycle, the higher particular levels seen in the cold start condition were not present since the vehicle was already warmed up, Fig. 15. Note that the ordinate of this figure has been expanded to only cover the range of 0 to 1.4 mg/m^3. These results emphasize the serious problem associated with cold start vehicle operation.

The highway fuel economy tests (HWFET) transient cycle particulate emissions results for two separate trials are shown in Fig. 16. Note the relatively large peaks in the emissions that correlate with each of the engine acceleration events. 100 pulse averages were used in recording these data after an elapsed time of 125 seconds, which resulted in a reduced temporal resolution of 5s. There is a general trend in these data for the second trial producing higher levels of carbonaceous particular emissions which could be due to number of factors including changes in the environmental conditions and variations in the driver performance from one day to the next.

Measurements using the ELPI instrument were made post dilution so the sampled stream experienced some cooling and consequently, the measured particulates are composed of carbonaceous materials and condensable organic species and trace elements. As previously stated, the ELPI instrument produces measurements at one-second intervals but appears to have a lower temporal response than the LII instrument. For the comparative results between the LII and ELPI instruments, the ELPI instrument results were summed over the 12 diameter stages to obtain the total number concentration of particles. The total number of particulates at each time interval was determined by multiplying the volume of an equivalent sphere having a diameter equal to the midpoint of each stage by the number of particles measured in each of the 12 stages. It was found that this result followed closely to the large size single stage results as might be expected since the larger particles dominate the total volume. Figure 17 shows a direct comparison of the results from the LII and ELPI instruments. The qualitative comparison of the particulate concentration measured by the LII instrument and the total volume measured by the ELPI instrument appears to correlate well with both following the driving cycle transients with similar relative magnitudes. A shorter but expanded time segment from Fig. 17 is shown in Fig. 18. The LII instrument reveals a better time response showing more detail in the record of the particulate loading as seen by the structure in the record. It also is evident that the ELPI instrument has a lower threshold limit below which it reports zero signal whereas the LII instrument is showing a nonzero particulate loading. It also appears that the ELPI instrument does not follow the rapid excursions in particle loading as seen around 190 to 200 seconds on the record shown in Fig. 18.

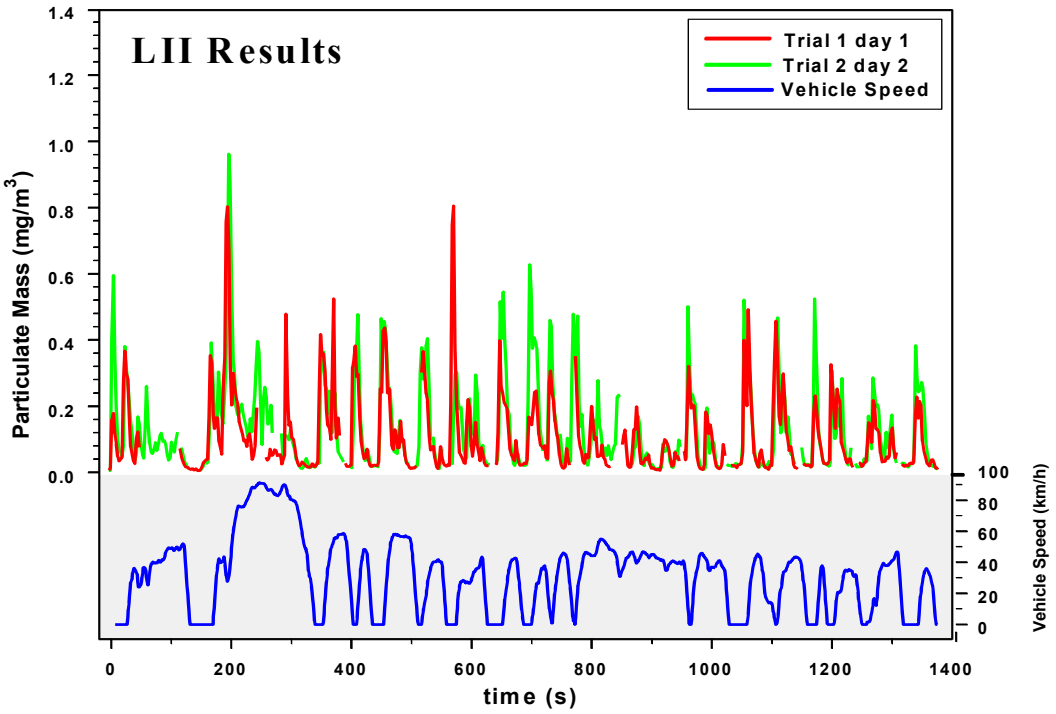

Figure 15: Comparison of hot start LA-4 transient cycle particulate mass emissions as determined by LII for two separate trials (top) and vehicle speed during LA-4 transient cycle (bottom).

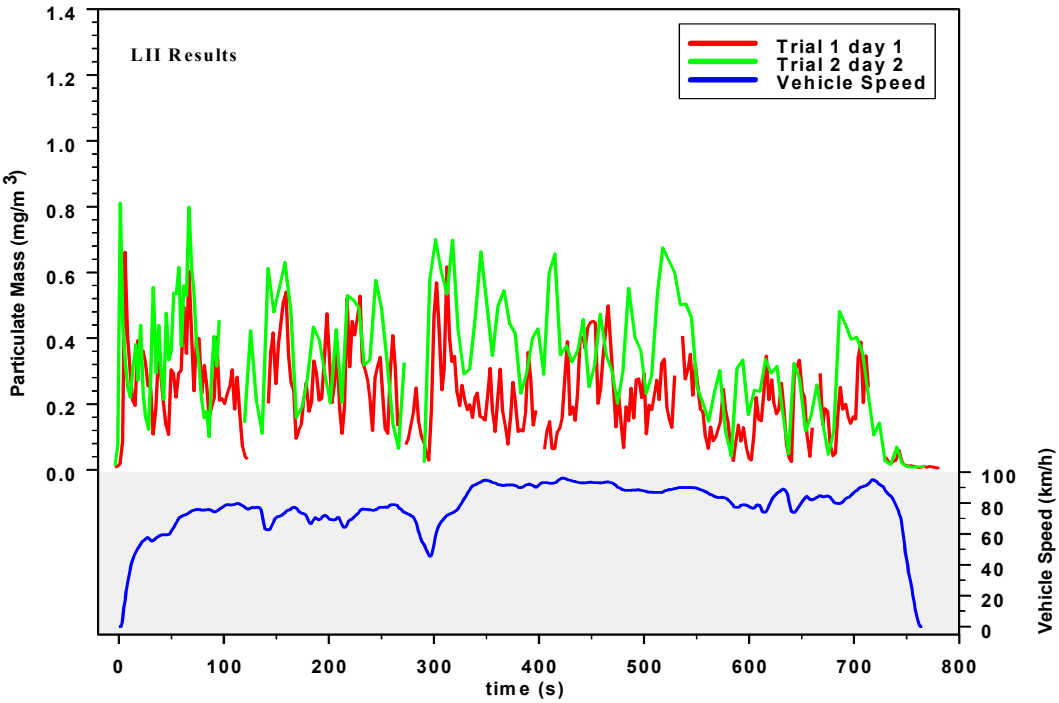

Figure 16: Comparison of HWFET transient cycle particulate mass emissions as determined by LII for two separate trials (top) and vehicle speed during HWFET transient cycle (bottom). Note that after 125 s, data for Trial 2 is based on 5 s averages.

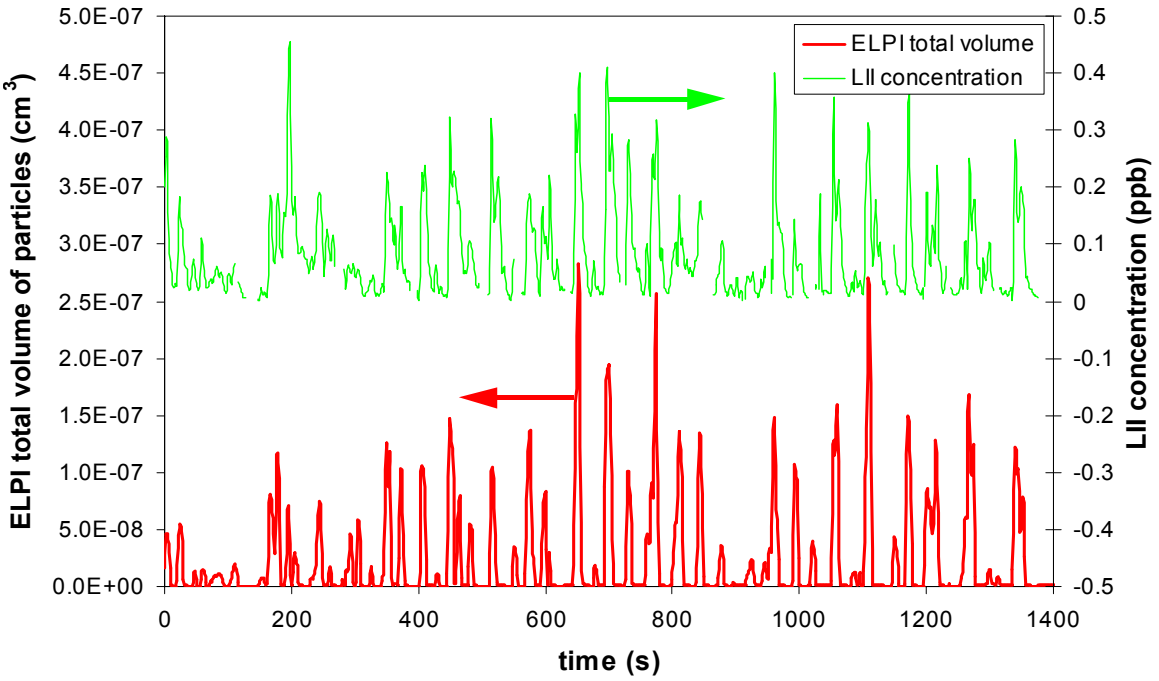

Figure 17: Comparison of particulate levels determined by LII (top) and ELPI (bottom) for hot start LA-4 transient cycle.

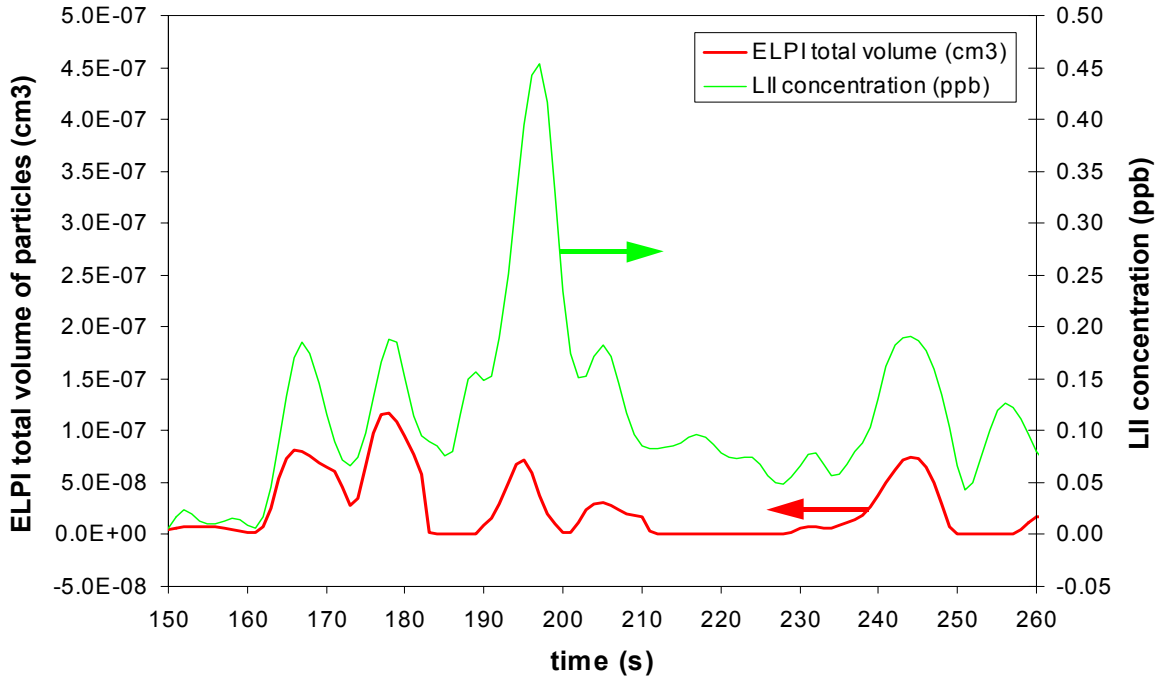

Figure 18: Detail from Figure 16 illustrating relative temporal response and sensitivity of LII and ELPI.

5. SUMMARY AND CONCLUSIONS

Laser-induced incandescence (LII) is a technique that has undergone extensive development and testing resulting in an instrument suitable for temporally and spatially resolved soot volume fraction particulate emissions characterizations. The theoretical development describing the high-energy pulsed laser heating of soot particles and their subsequent incandescence to obtain the primary soot particle size and volume fraction information was reviewed. Heat transfer theory for the nanometer sized particles undergoing heating and cooling over a period of nanoseconds was refined and the results summarized in this report. Since the method utilizes the measurement of the absolute incandescence intensity from the soot to obtain information on the soot volume fraction, a calibration method was required. A novel *in situ* approach has been developed and was summarized along with the theoretical justification of the method. The method utilizes a calibrated traceable light source of incandescence to characterize the light transmission as a function of wavelength for the optical components including the light filters in the receiver optics and also, the photodetectors.

A brief description of the LII instrument that is under development was provided. The instrument was designed to be compact and rugged with purge-protected optics and enclosure. Automated systems to control the laser fluence and incandescence signal to the detectors to allow ease of operation over a large range of soot concentrations have been developed and were incorporated along with the system software algorithms for their control. Signal processing systems and software have been developed to simplify the acquisition of the data and data reduction. Remote operation, data handling, and data storage may be handled over the Internet or other communications means.

The LII method has been thoroughly evaluated through experiments conducted in numerous practical environments. Measurements were performed in the exhaust of a single cylinder research diesel engine and compared to the gravimetric results obtained at a similar time and conditions. Measurements were also obtained with and AVL smoke meter. These results were in good agreement. Primary soot particle measurements were obtained using the LII signal decay rates. These results agreed with the trends in the data and showed very high precision but the accuracy was limited. Future work will be devoted to resolving the differences in the absolute primary particle size with the transmission electron microscope microscopy results. Small changes in the soot formation parameters could be detected as a change in the primary particle size using the LII approach.

Transient emissions measurements were performed on a direct injection spark ignition engine exhaust. Soot emissions were measured for the US EPA Cold Start, Hot Start, and Highway Fuel Economy Tests conditions. The results were compared to the ELPI (electric low pressure cascade impactor) instrument. The LII method had the advantage of not requiring dilution of the exhaust whereas the ELPI instrument required the incorporation of a mini-diluter to condition the sample before measurement. In general, the LII instrument tracked the transient soot emissions from the vehicle over the various driving cycles and showed good repeatability over similar test conditions. The LII instrument also showed better transient resolution and a significant advantage in the low emissions level detection and dynamic range.

6. ACKNOWLEDGEMENTS

The work of Artium Technologies was supported by the NASA Glenn Research Center SBIR Phase I and Phase II contracts and by the U.S. EPA under SBIR Phase I contract. The work at NRC Canada was partially funded by the Canadian Government's PERD Program.

7. REFERENCES

1. Arden, C., Burnett, R.T., Thun, M.J., Calle, E.E., Krewski, D., Ito, K., and Thurston, G.D., "Lung Cancer, Cardiopulmonary Mortality, and Long-term Exposure to Fine Particulate Air Pollution," JAMA, March 6, 2002, Vol. 287, No. 9.
2. Dobbins, R.A. and Megaridis, C.M., "Morphology of Flame-Generated Soot as Determined by Thermophoretic Sampling," Langmuir 3, 254-259, 1987.
3. Eckbreth, A. C., "Effects of Laser-Modulated Particulate Incandescence on Raman Scattering Diagnostics," Journal of Applied Physics, 48, pp.4473-4479, 1977.

4. Hofeldt, D.L., “Real-Time Soot Concentration Measurement Technique for Engine Exhaust Streams,” SAE Paper No. 930079, 1993.
5. Krishnan, S.S., Lin, K.-C., and Faeth, G.M., “Extinction and Scattering Properties of Soot Emitted from Buoyant Turbulent Diffusion Flames,” Journal of Heat Transfer, 123, pp.331-339, 2001.
6. Leroy, O., Perring, J., Jolly, J., and Pealat, M., “Thermal Accommodation of a Gas on a Surface and Heat Transfer in CVD and PECVD Experiments,” Journal of Physics D 30, 499-509, 1997.
7. Melton, L.A., “Soot Diagnostics based on Laser Heating,” Applied Optics, Vol.23, No. 13, 1984.
8. Smallwood, G. J., Snelling, D. R., Liu, F. and Gülder, Ö. L., “Clouds over Soot Evaporation: Errors in Modeling Laser-Induced Incandescence of Soot,” Journal of Heat Transfer, 123, pp. 814-818, 2001a.
9. Smallwood, G.J., Snelling, D.R., Gulder, Ö. L., Clavel. D., Gareau, D., Sawchuk, R.A., and Graham, L., “Transient Particulate Matter Measurements from the Exhaust of a Direct Injection Spark Ignition Automobile,” SAE Paper No. 2001-01-3581, 2001b.
10. Snelling, D.R., Smallwood, G.J., Campbell, I.G., Medlock, J.E., and Gulder, Ö. L., “Development and Application of Laser-Induced Incandescence (LII) as a Diagnostic for Soot Particulate Measurements,” AGARD 90th Symposium of the Propulsion and Energetics Panel on Advanced Non-Intrusive Instrumentation for Propulsion Engines, Brussels, Belgium, October 1997.
11. Snelling, D. R., Smallwood, G. J., Sawchuk, R. A., Neill, W. S., Gareau, D., Chippior, W. L., Liu, F., Gülder, Ö. L., and Bachalo, W. D., “Particulate Matter Measurements in a Diesel Engine Exhaust by Laser-Induced Incandescence and the Standard Gravimetric Procedure,” SAE Paper No. 1999-01-3653, 1999.
12. Snelling, D. R., Smallwood, G. J. and Gülder, Ö. L., “Absolute Light Intensity Measurements in Laser Induced Incandescence,” US Patent No. 6,154,277, 2000a.
13. Snelling, D. R., Smallwood, G. J., Gülder, Ö. L., Bachalo, W. D., and Sankar, S., “Soot Volume Fraction Characterization Using the Laser-Induced Incandescence Detection Method,” Proceedings of the 10th International Symposium on Applications of Laser Techniques to Fluid Mechanics, Lisbon, July, 2000b.
14. Snelling, D. R., Smallwood, G. J., Sawchuk, R. A., Neill, W. S., Gareau, D., Clavel, D., Chippior, W. L., Liu, F., Gülder, Ö. L. and Bachalo, W. D., “In-Situ Real-Time Characterization of Particulate Emissions from a Diesel Engine Exhaust by Laser-Induced Incandescence,” SAE paper 2000-01-1994, 2000c.
15. Snelling, D. R., Smallwood, G. J. Gülder, Ö. L., Liu, F., and Bachalo, W. D., “A Calibration-Independent Technique of Measuring Soot by Laser-Induced Incandescence Using Absolute Light Intensity,” The Second Joint Meeting of the US Sections of the Combustion Institute, Oakland, California, March 25-28, 2001.
16. Snelling, D.R., Thomson, K.A., Smallwood, G.J., Gulder, Ö. L., Weckman, E.J., and Fraser, R.A., “Spectrally Resolved Measurement of Flame Radiation to Determine Soot Temperature and Concentration,” AIAA Journal (in press), 2002.
17. Witze, P.O., “Diagnostics for the Measurement of Particulate Matter Emissions from reciprocating Engines,” The Fifth International Symposium on Diagnostics and Modeling of Combustion in Internal Combustion Engines (COMODIA), Nagoya, Japan, 2001.